Thermodynamic Stability of the Bacteriorhodopsin Lattice As Measured by Lipid Dilution†

Thomas A. Isenbarger‡ and Mark P. Krebs*,§

Department of Biomolecular Chemistry, University of Wisconsin Medical School, Madison, Wisconsin 53706-1532

Received April 2, 2001; Revised Manuscript Received July 5, 2001

ABSTRACT: To determine the strength of noncovalent interactions that stabilize a membrane protein complex, we have developed an in vitro method for quantifying the dissociation of the bacteriorhodopsin (BR) lattice, a naturally occurring two-dimensional crystal. A lattice suspension was titrated with a short- and long-chain phosphatidylcholine mixture to dilute BR within the lipid bilayer. The fraction of BR in the lattice form as a function of added lipid was determined by visible circular dichroism spectroscopy and fit with a cooperative self-assembly model to obtain a critical concentration for lattice assembly. Critical concentration values of wild-type and mutant proteins were used to calculate the change in lattice stability upon mutation ($\Delta\Delta G$). By using this method, a series of mutant proteins was examined in which residues at the BR−BR interface were replaced with smaller amino acids, either Ala or Gly. Most of the mutant lattices were destabilized, with $\Delta\Delta G$ values of 0.2−1.1 kcal/mol at 30 °C, consistent with favorable packing of apolar residues in the membrane. One mutant, I45A, was stabilized by ∼1.0 kcal/mol, possibly due to increased lipid entropy. The $\Delta\Delta G$ values agreed well with previous in vivo measurements, except in the case of I45A. The ability to measure the change in stability of mutant protein complexes in a lipid bilayer may provide a means of determining the contributions of specific protein−protein and protein−lipid interactions to membrane protein structure.

Many integral membrane proteins function as multimeric complexes, including bacterial and mammalian cytochrome oxidases (*1, 2*), potassium and mechanosensitive channels (*3, 4*), bacterial and plant light-harvesting and photosynthetic proteins (*5*−*7*), the mitochondrial F_1F_0 ATPase (*8*), and bacteriorhodopsin (*9*−*11*). A long-standing goal in identifying factors that stabilize such complexes has been to measure the strength of noncovalent protein−protein and protein−lipid interactions in the membrane. In principle, this goal might be achieved by thermodynamic analysis of mutations that affect the assembly of protein complexes of known structure, such as those cited above. However, progress has been limited due to the technical challenge of quantifying protein or lipid association in the membrane, which is necessary for thermodynamic analysis.

One approach to this challenge has been to approximate the membrane environment with detergents. This approach has been used extensively to study proteins with a single transmembrane segment (*12*−*14*), as exemplified by glycophorin A (GpA)[1] (*15, 16*). Typically, oligomerization of these proteins in sodium dodecyl sulfate (SDS) is monitored by SDS−PAGE to obtain a qualitative ranking of the effects of mutations in the transmembrane segment (*12, 13, 16, 17*). GpA dimerization in SDS has also been measured quantitatively by Förster resonance energy transfer (FRET) (*18*). However, the interpretation of protein oligomerization in SDS is complicated because the dissociation constants vary with detergent concentration (*18*) and because the oligomerization reactions equilibrate very slowly (*19*). Furthermore, the interaction of SDS with the protein may dominate the observed ΔG of dimerization (*18*), which might confound efforts to measure the energetic effects of mutations. For these reasons, more "membrane-like" zwitterionic and nonionic detergents have been used instead of SDS (*17, 18, 20, 21*). Significantly, it has been possible to determine the energetic effects of mutations on GpA dimerization in nonionic detergent by analytical ultracentrifugation (*20*). However, interpretation of $\Delta\Delta G$ values obtained under these conditions will require analysis of the multiple equilibria that influence protein oligomerization in detergent, including the association of detergent with itself and with the protein monomer and oligomer (*18*). Thus, although detergent-based approaches are highly promising, several issues must be addressed before they can be used to quantify the energetics of membrane protein assembly.

An alternative approach is to examine membrane protein assembly directly in the lipid bilayer. Methods are available

† T.A.I. was supported in part by a traineeship from NIH Molecular Biophysics Training Grant T32 GM08293. This work was partially funded by NSF Grants MCB 9514280 and MCB 9983120 to M.P.K. Circular dichroism data were obtained at the University of Wisconsin−Madison Biophysics Instrumentation Facility, which is supported by the University of Wisconsin−Madison and by NSF Grant BIR 9512577. Electron microscopy was performed at the University of Wisconsin Medical School Electron Microscope Facility.

* To whom correspondence should be addressed. E-mail: mpkrebs@ilstu.edu. Telephone: (309) 438-3834. Fax: (309) 438-3722.

‡ Present address: Department of Genetics, Harvard Medical School, Boston, MA 02114.

§ Present address: Department of Biological Sciences, Illinois State University, Normal, IL 61790-4120.

[1] Abbreviations: GpA, glycophorin A; FRET, Förster resonance energy transfer; BR, bacteriorhodopsin; BR_L, concentration of lattice BR; BR_T, concentration of total BR; CD, circular dichroism; PC, phosphatidylcholine; $diC_{14}PC$, 1,2-ditetradecanoyl-3-*sn*-phosphatidylcholine; diC_6PC, 1,2-dihexanoyl-3-*sn*-phosphatidylcholine; C_r, critical concentration; $\Delta\Delta G$, difference in the Gibbs free energy change.

10.1021/bi0106585 CCC: $20.00
Published on Web 09/06/2001

for examining protein oligomers in reconstituted lipid bilayers such as neutron diffraction and FRET (*19*, *22*−*24*). However, while these methods have been used to determine the number of subunits per oligomer, it has been more difficult to measure the distribution of monomeric and oligomeric forms required for determining an association constant. Another method is to examine oligomerization in vivo by expressing a transmembrane segment of interest covalently attached to a reporter domain such as the λ repressor or ToxR DNA binding domains (*21*, *25*, *26*). These strategies have been implemented to rank mutant phenotypes and thus define structural motifs that promote dimerization of transmembrane segments. Most of the mutant phenotypes assigned by this method correlated well with the results of studies in SDS (*25*, *26*). However, the in vivo phenotype of some mutations (*25*), particularly polar substitutions (*26*), did not agree with the in vitro measurements. This is likely due to differences in the interactions of detergents and bilayer lipids with proteins, and further emphasizes the importance of studying membrane protein complexes in a bilayer environment. Significantly, none of these approaches has yielded the thermodynamic values needed to quantify the interactions that stabilize a membrane protein complex in a lipid bilayer.

To study the stability of an integral membrane protein complex, we have chosen bacteriorhodopsin (BR), a seven-transmembrane α-helical protein that contains a covalently bound retinal cofactor. In *Halobacterium salinarum*, BR forms the purple membrane, a two-dimensional crystalline lattice of BR, and lipid molecules. High-resolution diffraction studies of the purple membrane (*27*, *28*) and three-dimensional crystals (*10*, *11*, *29*, *30*) have yielded the structure of BR and portions of the associated native lipids. Previously, we used these structures to identify amino acid residues within the lipid bilayer that appeared to make contacts at the interface between BR monomers. The contributions of these residues to lattice stability were tested with an in vivo assay based on BR cooperative self-assembly (*31*−*33*). Here, we have measured the thermodynamic stability of the BR lattice by a novel method in which the purified lattice is diluted with a synthetic lipid mixture, and the equilibrium distribution of BR in the lattice and monomeric forms was determined. We used this method to quantify the contributions of individual amino acid side chains to BR lattice stability within the lipid bilayer. The implications of this work for examining factors that stabilize membrane protein complexes are discussed.

EXPERIMENTAL PROCEDURES

Materials. Long- and short-chain phosphatidylcholines ($diC_{14}PC$ and diC_6PC, >99% pure) were purchased from Avanti Polar Lipids, Inc. (Alabaster, AL). Qorpak borosilicate glass vials with polytetrafluoroethylene-lined caps were used for sample preparation where noted.

Purification of BR Lattices and Titration with Lipid. BR lattices were purified from mutant *H. salinarum* strains as described previously (*32*), except that linear sucrose density gradients were created using a model 117 BioComp (Fredericton, NB) Gradient Mate. Gradient linearity was confirmed by measuring the refractive indices of gradient fractions on a Reichert-Jung Abbe Mark II digital refractometer. For lipid titrations, a phosphatidylcholine (PC) mixture was added to ∼0.5 mg/mL (18 μM) purified BR lattice in 50 mM HEPES (pH 6.9), 50 mM NaCl, and 0.025% (w/v) NaN_3. The PC mixture of $diC_{14}PC$ and diC_6PC (2:1, w/w) was mixed at 50 mg/mL total PC in water, and aliquots were stored at −70 °C. For each experiment, freshly thawed aliquots were diluted to 5 mg/mL. Additions were made to the individual samples from this working stock. Because this stock clouds in ∼1−2 h, all additions were made within 30 min of dilution. Samples (500 μL) were mixed in 1.5 mL polypropylene tubes or glass vials and incubated in the dark at 25 or 30 °C for ∼4 days to fully equilibrate the sample. Although incubation in glass or plastic does not affect the circular dichroism spectrum, incubation in glass yields more homogeneous samples as determined by centrifugation on sucrose gradients.

Density Measurements and Fitting. To determine the densities of the purified lattice, a 500 μL sample was applied to a linear (from 30 to 50%, w/w) isopycnic sucrose density gradient and centrifuged in an SW28.1 rotor at 27 000 rpm for 17 h at 15 °C. After fractionation in a 96-well plate, the BR peak was defined by measuring the absorbance at 562 nm of each fraction with an EL_x800 Universal Plate Reader (Bio-Tek Instruments, Inc., Winooski, VT). The data were fit with a Gaussian function, and the refractive indices of 7−10 fractions encompassing the peak were recorded at 20 ± 0.1 °C using the digital refractometer. These data were fit with a linear function to determine the refractive index and buoyant density at the peak. To determine the densities of samples incubated with PC, 500 μL samples were applied to linear 20 to 45% (w/w) isopycnic sucrose density gradients and fractionated as described above. To estimate the fraction of PC incorporated, the buoyant densities were plotted as a function of added PC and fit with the equation

$$\nu = f_0\nu_0 + f_{PC}\nu_{PC} \quad (1)$$

where ν, ν_0, and ν_{PC} are the partial specific volumes (1/density) of the PC-treated lattice, the untreated lattice, and the PC mixture, respectively, and f_0 and f_{PC} refer to the mass fractions of each component. The variable f_{PC} is defined as the product of the added PC concentration and a constant reflecting the fraction of added PC that is incorporated into the membranes. For fitting the density data, a value of 0.938 mL/g is used for ν_{PC}. This value is a weighted average calculated from a value of 0.865 mL/g for diC_6PC (*34*) and a value of 0.964 mL/g for $diC_{14}PC$ determined from interpolating a three-term polynomial fit of partial specific volume versus chain length for PC (*34*).

Electron Microscopy. A plastic film-coating solution was prepared prior to staining using 0.40% Pioloform (Ted Pella, Inc., Redding, CA) dissolved in $CHCl_3$. Clean glass slides were dipped in a prepared solution, stripped, and floated on distilled water. Precleaned 400 mesh Cu grids were placed on the floating film and picked up with a piece of Parafilm. The sample was mixed with three parts of 2.0% $(NH_4)_2MoO_4$ (pH 7.2) as described in the One-Step Method (*35*) and vortexed for 10 s. The sample and stain mixture was then placed on a prepared Pioloform-coated grid opposite the coated side. The mixture was allowed to adsorb for 1 min and any excess wicked away. The stained sample was then viewed at 80 kV on a Philips CM120 electron microscope in the conventional bright field transmission mode.

Circular Dichroism and Absorption Spectroscopy. Circular dichroism (CD) spectra were recorded on an Aviv (Lakewood, NJ) 202SF circular dichroism spectrometer using a 1 cm path length quartz microcell. Single scans were recorded at 25 or 30 °C, using a 1 s averaging time, a 1 s settling time, a 1 nm bandwidth, and a 2 nm sampling interval, and baseline corrected with a water blank. Both lattice and monomer forms of BR are spectrally well-behaved in that the CD signal is linearly related to concentration over the range of added PC tested (0.0−1.5 mg/mL). To determine BR concentrations, UV−visible absorption spectra were collected at room temperature on a Perkin-Elmer Lambda 2 spectrophotometer using a 1 cm path length cell. Prior to CD or absorption spectroscopy, samples were illuminated in >530 nm light for ∼5 min to adapt BR to light.

Critical Concentration Determination and ΔΔG Calculation. In PC titrations, the concentration of BR in the lattice form decreases as PC is added, while the total concentration of BR is constant. The CD spectra were treated as a linear combination of the two end-point spectra, which are defined as the spectrum of the untreated lattice and the spectrum of the monomer titration end point at ≥1 mg/mL of added PC. The ellipticity at any wavelength is then given by

$$e = f_L e_L + f_M e_M + C \quad (2)$$

where e is the ellipticity of the sample at any wavelength, e_L and e_M are the ellipticities of the lattice and monomer end-point spectra at the same wavelength, respectively, f_L and f_M are the fractional contributions of the lattice and monomer spectra, respectively, and C is a constant to account for small offsets among the spectra attributed to baseline drift in the spectrometer. The concentration of BR in the lattice form (BR_L) is the product of the total BR concentration (BR_T) and f_L. For critical concentration plots, BR concentrations are described as a BR:lipid ratio in units of moles per mole. Plots of BR_L versus BR_T are fit with a self-assembly model to determine the critical concentration (C_r) for lattice formation (*32*):

$$BR_L = 0 \text{ if } BR_T < C_r;\ BR_L = BR_T - C_r \text{ if } BR_T = C_r \quad (3)$$

To calculate differences in the Gibbs free energy change of association caused by an amino acid substitution ($\Delta\Delta G$), the experimentally determined C_r values for wild-type and mutant BR lattices were used to calculate $\Delta\Delta G$ in the equation

$$\Delta\Delta G = -RT \ln(C_{r,wt}/C_{r,m}) \quad (4)$$

where $C_{r,wt}$ and $C_{r,m}$ are the critical concentration values for the wild-type and mutant lattices, respectively.

RESULTS

Experimental Rationale. One approach to measuring the thermodynamic stability of a protein complex is to examine dissociation of the complex by dilution. The decrease in the concentration of an aqueous−soluble complex upon dilution in buffer is measured as a function of the total protein concentration, and a dissociation constant is calculated. We have developed an analogous "lipid dilution" approach for measuring the stability of the BR lattice. An aqueous suspension of the purified BR lattice is combined with a mixture of short- and long-chain PC under conditions in which vesicle formation occurs. The total concentration of BR per unit volume in the sample remains constant, but the concentration of BR within the lipid environment decreases. By monitoring the dissociation of the BR lattice as a function of PC concentration, we can determine the equilibrium constant for lattice assembly. Significantly, this approach allows membrane protein interactions to be analyzed in a lipid environment.

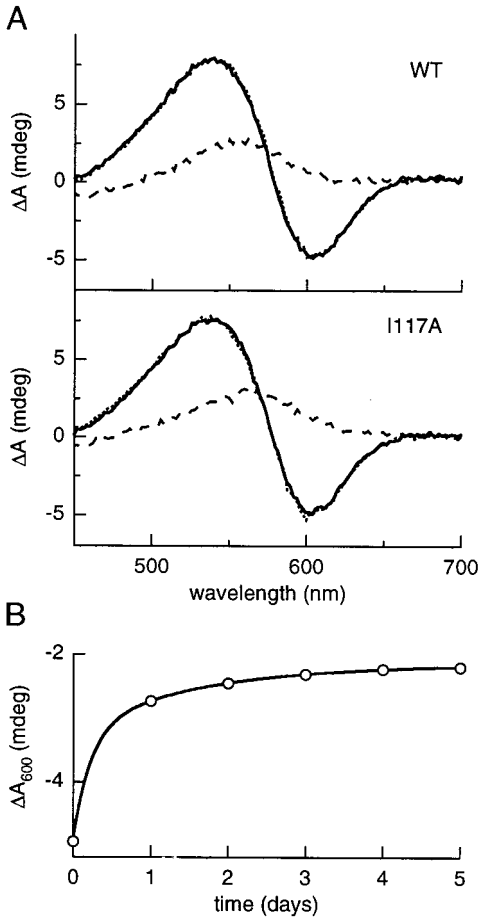

FIGURE 1: Treatment of the BR lattice with the PC mixture. (A) Circular dichroism spectra of 0.5 mg/mL suspensions of wild-type and I117A lattices before (solid line) and after incubation at 30 °C with 0.33 mg/mL diC_6PC alone (dotted line) or in combination with 0.66 mg/mL $diC_{14}PC$ (dashed line, 1.0 mg/mL total PC). Samples were suspended in 50 mM HEPES (pH 6.9), 50 mM NaCl, and 0.025% (w/v) NaN_3. (B) Equilibration time course at 30 °C of the wild-type lattice treated with a 0.25 mg/mL PC mixture. Data are fit with a monoexponential function.

Conversion of the BR Lattice to Monomeric BR with an Added PC Mixture. Mixtures of short- and long-chain phosphatidylcholine (PC) have been used previously to study the structure and function of BR and other membrane proteins (*36*, *37*) and are attractive for the lipid dilution approach because of their tendency to form bilayer structures such as bicelles or vesicles (*38*, *39*). To demonstrate the feasibility of diluting the BR lattice with PC, lattice purified from wild-type and I117A cells was mixed with a 1 mg/mL PC mixture (2:1 $diC_{14}PC/diC_6PC$, w/w) and examined by circular dichroism (CD) spectroscopy (Figure 1A). The I117A mutant was chosen because it was previously shown to destabilize the lattice (*31*, *32*) and would therefore provide a good test of assay conditions. The visible CD spectrum of the untreated purified BR lattice displays a biphasic feature

(Figure 1A, solid line). It is generally accepted that this feature is due to intra- and intertrimer exciton coupling among the regularly arranged BR chromophores in the lattice (*40*). When the lattice is equilibrated with 1 mg/mL PC, the visible CD spectrum possesses a single positive peak (Figure 1A, dashed line) consistent with monomeric BR (*40*−*42*). UV−visible absorption spectroscopy of PC-treated samples revealed a peak near 560 nm, indicating that BR tertiary structure was not grossly altered by the added lipid (data not shown). However, the PC-treated samples exhibited an ∼10% decrease in the extinction coefficient and an ∼10 nm blue shift in the absorbance maximum (data not shown). These spectral shifts have been observed previously upon conversion of the lattice into BR monomers in $diC_{14}PC$ (*41*), suggesting that the protein is monomeric under our conditions. There was no evidence of an absorption peak at 380 nm, suggesting that PC-treated samples lacked free retinal and that BR was not bleached. Thus, incubation with the PC mixture dissociates the BR lattice into monomers without otherwise affecting the structure of the protein.

To determine if the conversion of the lattice to monomeric BR is due to diC_6PC alone, wild-type and I117A lattices were treated with 0.33 mg/mL diC_6PC, the same concentration as in the 1.0 mg/mL PC mixture. The CD spectra of treated and untreated samples were the same (Figure 1A, compare the solid and dotted lines), indicating that diC_6PC alone does not disrupt the lattice. The effect of $diC_{14}PC$ alone could not be determined since it is virtually insoluble in aqueous buffer and results in a heterogeneous cloudy suspension in the absence or presence of the BR lattice. Thus, conversion of lattice BR to monomers requires both the long-chain PC, presumably to integrate into and extend the BR lattice bilayer, and the short-chain PC, to solubilize the long-chain PC.

To determine if PC treatment results in solubilization of the lattice as observed with the nonionic detergents Triton X-100 and octyl glucoside (*43*), samples incubated with 1 mg/mL PC were centrifuged at 200000*g* for 45 min, which is typically used to separate detergent-solubilized BR from unsolubilized material (*44*). After centrifugation, >97% of the BR was present in the compact purple pellet, as determined from the absorption spectra of samples before and after centrifugation (data not shown). Thus, incubation with PC converts lattice BR to monomeric BR without solubilization of the membrane.

Equilibration of the Lattice with PC. Before further characterization of the BR−lipid aggregates and initiation of thermodynamic studies, it was necessary to ensure that measurements were made under equilibrium conditions. To determine the time required for the added PC to equilibrate, lattices were treated with the minimum amount of PC that produces a detectable change in the CD spectrum at 600 nm. Greater amounts of PC are expected to equilibrate more rapidly. Individual samples were incubated for 0−5 days at 30 °C before CD spectra were recorded. A fit of the CD data with a monoexponential function indicated that within 4 days the samples reach 90−99% of the plateau ellipticity value at 600 nm predicted from the fit (Figure 1B). Thus, an incubation of 4 days appeared to be sufficient for equilibration of PC-treated samples and was used routinely prior to performing CD spectroscopy and control experiments.

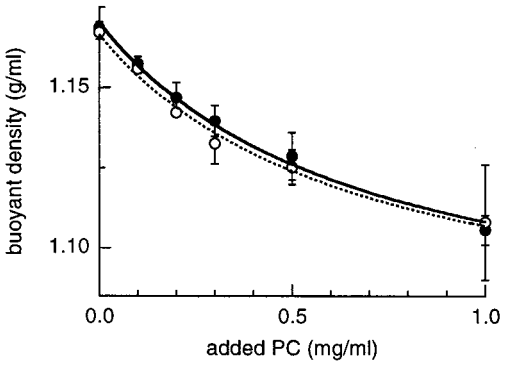

FIGURE 2: Density analysis of BR lattices. Plots of specific gravity vs the amount of PC added for the wild type (●) and I117A (○). The data points and error bars represent the means and standard deviations, respectively, from three independent determinations. The data are fit with eq 1 (see Experimental Procedures; wild type, solid line; I117A, dashed line).

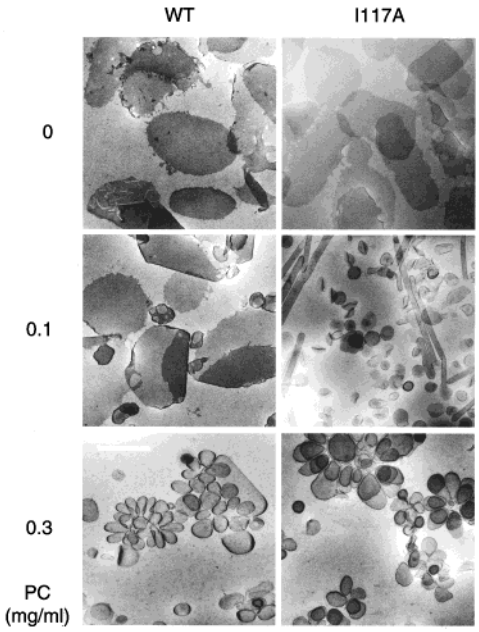

FIGURE 3: Electron micrographs of wild-type and I117A lattices before (0) and after incubation with 0.1 and 0.3 mg/mL PC. A distance of 0.5 μm is indicated by the white bar.

Lipid Treatment Decreases the Density of BR Lattice Membranes. The results described above are consistent with incorporation of PC into the purified lattices, resulting in a decrease in the protein:lipid ratio within the bilayer that dissociates the BR lattice. To provide further evidence of PC incorporation, we determined whether the buoyant density of the lattice decreased with added PC. BR lattices were treated with increasing amounts of PC, incubated for 4 days, and centrifuged to equilibrium on sucrose density gradients. The gradients were fractionated, and the buoyant densities of the BR-containing fractions were determined. The buoyant densities of the untreated BR lattices ranged from 1.171 to 1.179 mg/mL with errors from 0.0001 to 0.0068 mg/mL, close to the previously reported value of 1.18 mg/mL (*45*). The buoyant densities of the wild-type and I117A membranes decreased with added PC to ∼1.11 mg/mL at the highest PC concentration [Figure 2(● and ○, respectively)].

To estimate the extent of PC incorporation, the density data were fit with eq 1, which accounts for the partial specific volumes of the BR lattice and added PC mixture (see

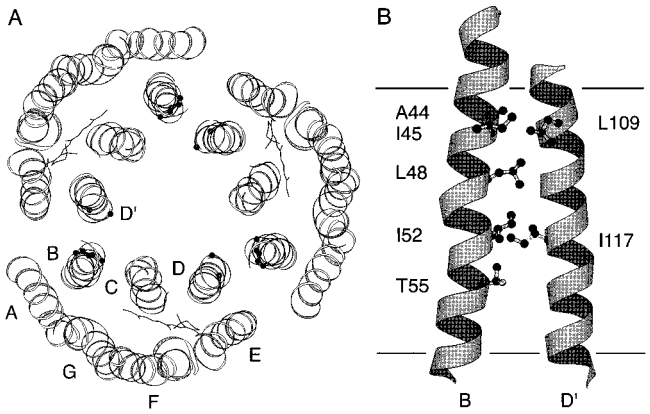

FIGURE 4: Locations of substitutions. (A) The helices and retinal cofactors of a BR trimer are viewed normal to the membrane from the cell interior. The helices of one monomer are labeled A−G. Residues (●) at the BR−BR interface are located on helix B from one BR monomer (from left to right, I45, I52, L48, T55, and A44) and on helix D′ from a neighboring monomer (from left to right, I117 and L109). (B) Helices B and D′ are shown as viewed within the membrane core from the center of a BR trimer. The substituted residues are drawn in ball-and-stick representations and labeled; the boundaries of the apolar membrane core are designated with horizontal lines.

Experimental Procedures). The data are reasonably fit with a model that assumes a constant mass fraction of the added PC is incorporated at all PC concentrations (Figure 2). In the curves that are shown, the fraction incorporated corresponds to $^2/_3$ of the added PC. This result is consistent with complete incorporation of the long-chain lipid, diC_{14}PC, which composes $^2/_3$ of the PC mixture by mass and is much more hydrophobic than the short-chain lipid. Although other interpretations are possible, it is significant that identical results were obtained for I117A under the same conditions. Thus, it is reasonable to assume that the incorporation of PC into wild-type and mutant lattices is similar.

Examination of Samples by Electron Microscopy. To determine whether membrane-like structures were present in samples treated with PC, samples were stained and examined by electron microscopy. Untreated lattices purified from the wild type and I117A appear as roughly circular or oval membrane sheets ∼0.5−1.0 mm in diameter (Figure 3, 0 mg of PC/mL). Upon titration with PC, the membrane sheets are gradually replaced by unilamellar vesicles with a diameter of ∼0.1 μm at intermediate PC concentrations and ∼0.3−0.5 μm at higher concentrations (Figure 3, 0.1 and 0.3 mg of PC/mL). In the case of the I117A mutant, unilamellar tube structures are sometimes seen at intermediate PC concentrations (Figure 3, 0.1 mg of PC/mL). When samples are prepared without the BR lattice, no vesicular structures are detected (data not shown). Thus, titration of the BR lattice with the PC mixture results in the conversion of the BR lattice into other unilamellar bilayer structures.

Lipid Dilution of BR Mutants. We previously described a series of BR mutants containing single Ala and Gly substitutions at the interface between transmembrane helices in neighboring BR monomers (Figure 4) (*32*). To test the stability of lattices comprising these mutant proteins by lipid dilution, wild-type and mutant lattices were purified and titrated with the PC mixture. Single CD scans of each titration sample were acquired, and the spectra from each titration series were plotted together (Figure 5). With this approach, small variations in the spectrometer baseline were sometimes observed (see below). The data may have been improved by obtaining multiple scans and averaging them, but this was impractical because of the large number of samples.

For all mutants and the wild type, the CD (Figure 5) and absorption spectra (data not shown) of both titration end points are consistent with BR in lattice and monomeric forms. A single isodichroic point at ∼570 nm is readily observed in most of the titrations (WT, A44G, T55A, L109A, and I117A in Figure 5). In the remaining titrations, an isodichroic point is not observed due to the presence of one or more spectra that appear to be shifted due to a displacement of the spectrometer baseline (I45A, L48A, and I52A in Figure 5). For example, one spectrum in the L48A titration series showed a non-zero ellipticity at 650−700 nm where BR absorbs very little and the ellipticity should be zero, indicating that the instrument baseline was shifted (Figure 5).

The baseline shift was corrected by fitting the raw data with a linear combination of end-point spectra using eq 2, which includes an offset term for the baseline variations (Figure 6). All of the data in Figure 5 were treated with this method. In all cases, the fits displayed excellent agreement with the data, as shown for the wild type and I52A in Figure 6, indicating that two states, lattice and monomer, are sufficient to account for the spectra and that significantly populated or spectroscopically active intermediates are absent. Thus, the mutant and wild-type lattices all undergo similar conversion to monomeric BR when titrated with PC.

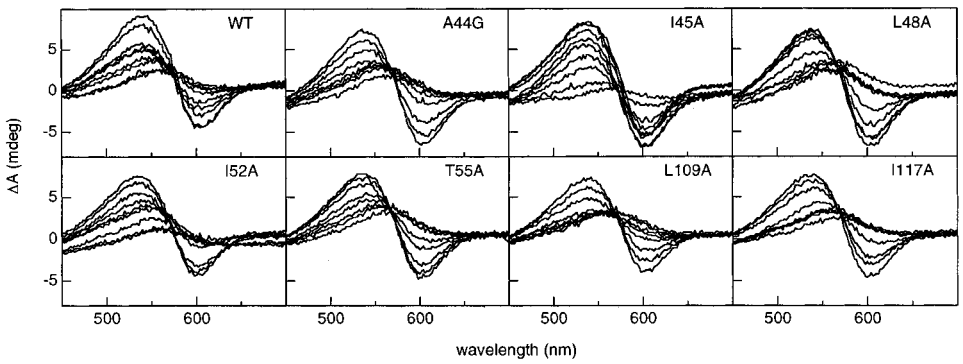

FIGURE 5: Lipid titrations for wild-type and mutant BR lattices. Circular dichroism spectra of 0.5 mg/mL lattice incubated with the following concentrations of the PC mixture: 0, 0.1, 0.2, 0.25, 0.3, 0.5, 0.7, 1.0, and 1.5 mg/mL for the wild type, A44G, I45A, I52A, T55A, and L109A and 0, 0.02, 0.05, 0.1, 0.15, 0.25, 0.3, 0.5, 1.0 mg/mL for L48A and I117A. No corrections are made for baseline variations within a titration series, or for small (<10%) differences in the starting BR concentrations among series.

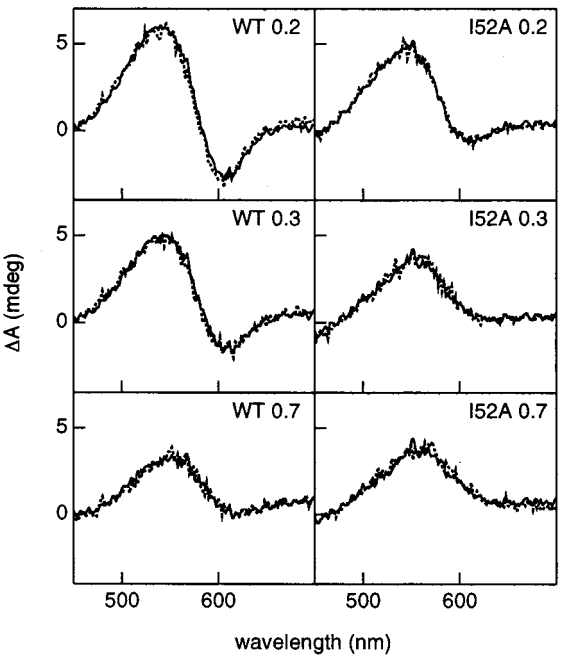

FIGURE 6: Representative fits of CD data. The raw CD spectrum (dotted line) and fits (eq 2, solid line) are shown for wild type (left column) and I52A (right column) at 0.2, 0.3, and 0.7 mg/mL PC. The I52A spectrum at 0.7 mg/mL is one that displays a baseline shift in Figure 5.

Determination of C_r and $\Delta\Delta G$ for the BR Lattices. In earlier studies of BR lattice stability (*32*), the accumulation of the BR lattice in vivo was modeled as a cooperative self-assembly process. This allowed us to derive the critical concentration (C_r) for BR assembly. C_r is the minimal concentration of total protomer required to initiate formation of the polymer and is equivalent to $1/K_{app}$, where K_{app} is the apparent equilibrium constant for addition of protomers to the polymer (*46*). Thus, mutants that disrupt the lattice are expected to exhibit a higher C_r than wild-type BR.

A similar analysis was applied to compare the stabilities of wild-type and mutant BR lattices assayed by lipid dilution in vitro. For each PC-treated sample, the CD spectrum (Figure 6, dotted line) was fit with eq 2 (Figure 6, solid line) to determine BR_L, which was graphed versus BR_T to determine C_r values (Figure 7). The C_r is defined as the lowest value of BR_T at which lattice is present, represented by a change in the slope of the self-assembly function (eq 3) from 0 to 1 (Figure 7) (*32*). The self-assembly model used for the fits assumes that PM lipids remain bound to dissociated BR monomers and therefore are not included in calculating the total lipid concentration. When PM lipids were treated as bulk lipid, the fits were significantly worse (data not shown). When the data are fit in this manner, all samples demonstrated a good fit to the self-assembly model and significant differences in C_r were detected (Figure 7). The C_r values for all the mutants were first determined in this manner by in vitro PC titration at 25 °C (Table 1). C_r was also determined at 30 °C (Table 1) to avoid potential artifacts at 25 °C, which is near the lamellar gel to liquid crystal ($P_\beta \rightarrow L_\alpha$) transition temperature of $diC_{14}PC$ of 23.6 ± 1.5 °C (*47*). As expected, the C_r values are higher at 30 °C than at 25 °C (Table 1).

Using the C_r values and eq 4, $\Delta\Delta G$ values were calculated for each mutant at 25 °C (Figure 8, gray bars) and at 30 °C

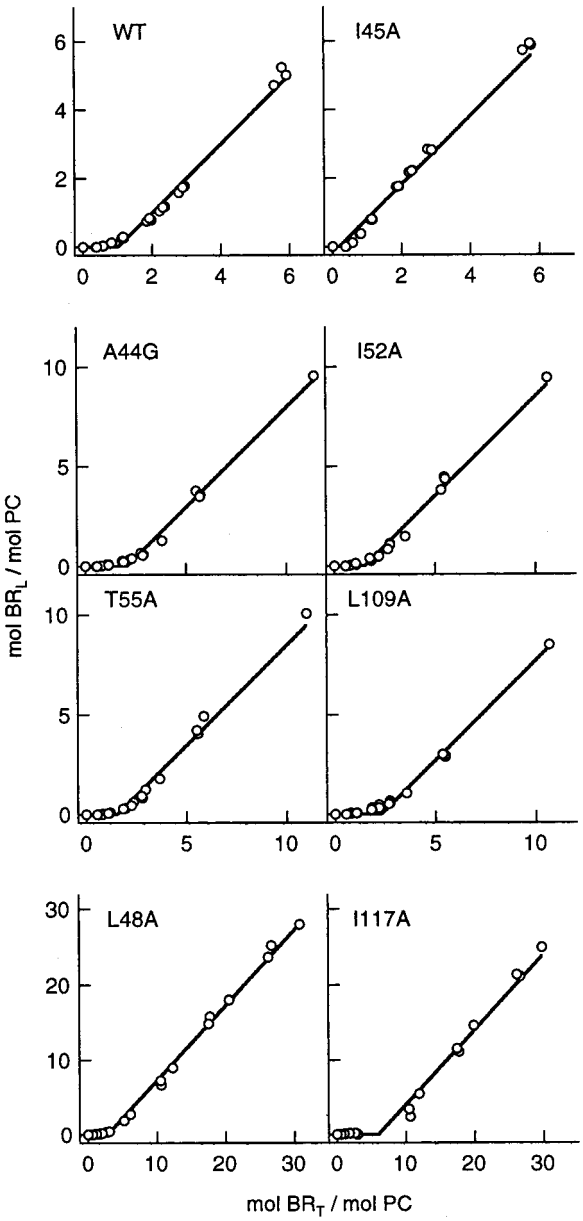

FIGURE 7: Critical concentration plots for wild-type and mutant BR lattices. Using the PC titration data (Figure 5), the amount of BR in the lattice form is calculated and plotted vs the total amount of BR in the sample. The data are fit with a self-assembly model to determine C_r (solid curves).

Table 1: C_r Values of Mutants (moles of BR per mole of lipid)[a]

	25 °C	30 °C		25 °C	30 °C
wild type	0.43 ± 0.08	1.03 ± 0.06	I52A	1.18 ± 0.21	1.53 ± 0.05
A44G	1.44 ± 0.27	2.05 ± 0.22	T55A	0.93 ± 0.28	1.56 ± 0.12
I45A	0.15 ± 0.02	0.21 ± 0.03	L109A	1.12 ± 0.25	2.26 ± 0.12
L48A	2.29 ± 0.67	2.80 ± 0.30	I117A	4.13 ± 1.69	6.10 ± 0.66

[a] Values and errors are the means and standard deviations, respectively, from three independent experiments.

(Figure 8, black bars). Nearly all the substitutions destabilize the BR lattice, with positive $\Delta\Delta G$ values of 0.4−1.3 kcal/mol at 25 °C and 0.2−1.1 kcal/mol at 30 °C, with errors from 0.04 to 0.15 kcal/mol at 25 °C and from 0.03 to 0.09 kcal/mol at 30 °C. The I45A substitution resulted in a lattice that is more stable than the wild type by 0.6−1.0 kcal/mol. For comparison, we calculated $\Delta\Delta G$ values from C_r values previously determined in vivo for the same mutants (Figure

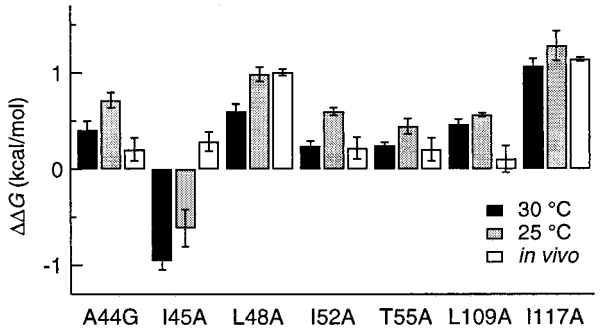

FIGURE 8: Comparison of $\Delta\Delta G$ values. Using the C_r values determined from PC titrations at 25 and 30 °C, the $\Delta\Delta G$ for each substitution that was examined was calculated. Values and error bars represent the means and standard deviations, respectively, from three independent determinations. These in vitro values are compared with $\Delta\Delta G$ values calculated from the C_r values determined in vivo (*32*). The in vivo errors are calculated by standard error propagation methods using the errors in the C_r values (*32*).

8, white bars) (*32*). The in vivo values show similar trends, though some differences are apparent (see Discussion).

DISCUSSION

While many previous approaches have been used to assess the assembly of integral membrane protein complexes, none has evaluated the thermodynamic stability of a membrane protein complex in the context of a lipid bilayer. In the assay of thermodynamic stability we have described here, the BR lattice is equilibrated with a PC mixture that dilutes the lattice and promotes its dissociation. Similar mixtures of long- and short-chain PC have been shown to spontaneously form unilamellar vesicles (*48*) and "bicelles" (*39*), and have been used for the reconstitution of integral membrane proteins, including BR (*36*, *37*). The added lipid is associated with the lattice, as demonstrated by a steady decrease in the buoyant density of the BR sample with increasing levels of PC and by the progressive replacement of the intact lattice with vesicles as determined by electron microscopy. As in the in vivo assay we described previously (*32*), a self-assembly model is used to determine the C_r for lattice assembly, which is then used to calculate $\Delta\Delta G$. We used this method to quantify the contributions to the free energy of assembly made by individual amino acid side chains at a protein−protein interface within the membrane bilayer.

Our spectroscopic data support a two-state equilibrium between the BR lattice and BR monomers. Two spectroscopic states are indicated by the existence of a single isodichroic point, which is apparent in most of the CD titration series (Figure 5) and implied by the good fits of all titration series with a two-state model that includes an offset for baseline shifts (Figure 6). We favor the explanation that the end point observed at high PC concentrations is monomeric BR, similar to that observed in previous studies of PM solubilization and reconstitution in lipid bilayers (*40*−*42*). However, it is formally possible that this end point may be a BR trimer, since the spectroscopic characteristics of the isolated trimer have not been established in this or previously published work. In the unlikely case that the end point consists of BR trimers, the $\Delta\Delta G$ measurements would still reflect the effects of the amino acid substitutions on BR−BR interactions. It is also possible that trimeric BR exists as an intermediate in the conversion of lattice BR to monomers. In cooperative self-assembly, oligomeric intermediates are predicted to be present at very low concentrations under equilibrium conditions and do not affect the determination of C_r (*49*). If trimeric intermediates were present in our experiments at appreciable levels, the relationship between the total BR and lattice BR concentrations (Figure 7) would deviate significantly from the cooperative self-assembly model. Because the titration data are fit well with this model (Figure 7), any intermediate forms must be present at low levels.

To fit the titration data to the self-assembly model, it was necessary to assume that the native lipids associated with BR in the lattice remain tightly bound to BR monomers in the synthetic lipid bilayers and can therefore be omitted from the calculation of total lipid concentration. In support of this assumption, (i) endogenous archaeal lipids often remain bound to BR when the lattice is solubilized in nonionic detergents (*50*, *51*) and (ii) the BR structural models include highly ordered lipids (*10*, *11*, *27*−*30*) which have been modeled to interact preferentially with BR in silico (*52*). Tight association of lipids with membrane proteins is not uncommon, as specific lipid interactions have also been suggested to support the structure and function of many other membrane proteins (*53*−*55*). Thus, our data best describe a system in which a monomeric BR−archaeal lipid complex is in equilibrium with the BR lattice.

The simplest interpretation of the positive $\Delta\Delta G$ values is that they represent the extent to which the side chains participate in stabilizing interactions in the wild-type BR lattice. Values for $\Delta\Delta G$ are in the range of 0.4−1.3 kcal/mol at 25 °C and 0.2−1.1 kcal/mol at 30 °C. This agrees with previous measurements of the contributions that single side chains make toward membrane protein oligomerization in detergent (*20*). The residues examined form part of a tightly packed apolar surface at the BR−BR interface within the hydrocarbon core of the membrane. Thus, it is likely that substitutions in smaller side chains disrupt the lattice by removing favorable van der Waals interactions between these surfaces. Although it is possible that substitutions at the protein−protein interface could destabilize the lattice by favoring interactions with the added PC, this is unlikely because similar treatment with *H. salinarum* lipids produces the same trend in lattice stability as PC (T. A. Isenbarger and M. P. Krebs, unpublished results). These observations support a growing body of evidence which shows that van der Waals interactions within the hydrocarbon core of the membrane stabilize membrane protein assembly (*20*). However, protein−lipid and protein−protein interactions involving residues outside this region have been suggested to be important for stability (for a review, see ref *33*) and must be quantified to advance our understanding.

A surprising result is that replacing Ile45 with Ala (I45A) results in a lattice that is more stable by ~0.6−1.0 kcal/mol than the wild-type lattice. Although the cause of this increased stability is not currently known, it may be that the I45A substitution allows more freedom for nearby lipids, allowing an entropy gain, or that side chain rearrangements that strengthen BR−BR interactions occur. Stabilizing mutations may be fairly common among membrane proteins, as indicated by the finding that ~10% of unselected substitutions in diacylglycerol kinase stabilize oligomers of this protein (*56*). Like the diacylglycerol kinase oligomer, the

native BR lattice may not be optimized for stability, possibly because membrane proteins are stabilized during evolution by the minimum amount needed to allow folding and assembly in the lipid environment, or because a certain amount of destabilization is required for efficient function. High-resolution structural studies are probably needed to best explain these effects.

We compared the $\Delta\Delta G$ values with previous in vivo measurements of BR lattice stability to assess the physiological relevance of the in vitro results. The magnitudes of the in vitro and in vivo $\Delta\Delta G$ values are comparable, although the values determined in vitro are generally larger by as much as 0.5 kcal/mol. As discussed previously (*32*), in vivo estimates of $\Delta\Delta G$ may be biased by difficulties in measuring C_r for wild-type and mutant proteins that do not disrupt the lattice because accurately quantifying small amounts of nonlattice BR is hindered by the presence of other cellular pigments. The in vitro assay provides an accurate wild-type C_r value and therefore enables better estimation of $\Delta\Delta G$ for the mutants. The in vivo assay suggested that only two positions (Leu48 and Ile117) at the protein−protein interface contribute significantly (∼1.0 kcal/mol) to BR lattice stability (Figure 8). The in vitro data support the important role of these two amino acid side chains, but also suggest that the other side chains make a more significant contribution than suggested previously by the in vivo assay (Figure 8). The in vitro assay suggests that the I45A lattice is more stabilized than the wild-type lattice, whereas the in vivo results indicate that this substitution may be slightly destabilizing. Further improvements in the in vivo assay will be required to detect mutants that are more stable than the wild type.

The lipid dilution method developed here is a new tool for understanding the fundamentals of membrane protein assembly. For BR, targeted or random mutants can now be quantified in a lipid bilayer environment to reveal how different regions of the protein contribute to stability. The lipid composition of the system may also be controlled so that the roles of native archaeal lipids can be determined. The method may prove to be useful for examining the protein and lipid determinants required for the stability of other membrane protein complexes. The information gathered from these studies is expected to provide a basis for predicting membrane protein structure and stability.

ACKNOWLEDGMENT

We thank Darrell McCaslin for aid in circular dichroism spectroscopy, Juan de Pablo for critical comments, Randy Massey for electron microscopy, and Anant Menon and Ron Peck for comments on the manuscript.

REFERENCES

1. Iwata, S., Ostermeier, C., Ludwig, B., and Michel, H. (1995) *Nature 376*, 660−669.
2. Tsukihara, T., Aoyama, H., Yamashita, E., Tomizaki, T., Yamaguchi, H., Shinzawa-Itoh, K., Nakashima, R., Yaono, R., and Yoshikawa, S. (1996) *Science 272*, 1136−1144.
3. Doyle, D. A., Cabral, J. M., Pfuetzner, R. A., Kuo, A., Gulbis, J. M., Cohen, S. L., Chait, B. T., and MacKinnon, R. (1998) *Science 280*, 69−77.
4. Chang, G., Spencer, R. H., Lee, A. T., Barclay, M. T., and Rees, D. C. (1998) *Science 282*, 2220−2226.
5. Koepke, J., Hu, X. C., Muenke, C., Schulten, K., and Michel, H. (1996) *Structure 4*, 581−597.
6. Kühlbrandt, W., Wang, D. N., and Fujiyoshi, Y. (1994) *Nature 367*, 614−621.
7. McDermott, G., Prince, S. M., Freer, A. A., Hawthornthwaite-Lawless, A. M., Papiz, M. Z., Cogdell, R. J., and Isaacs, N. W. (1995) *Nature 374*, 517−521.
8. Stock, D., Leslie, A. G., and Walker, J. E. (1999) *Science 286*, 1700−1705.
9. Kimura, Y., Vassylyev, D. G., Miyazawa, A., Kidera, A., Matsushima, M., Mitsuoka, K., Murata, K., Hirai, T., and Fujiyoshi, Y. (1997) *Nature 389*, 206−211.
10. Belrhali, H., Nollert, P., Royant, A., Menzel, C., Rosenbusch, J. P., Landau, E. M., and Pebay-Peyroula, E. (1999) *Structure 7*, 909−917.
11. Essen, L.-O., Siegert, R., Lehmann, W. D., and Oesterhelt, D. (1998) *Proc. Natl. Acad. Sci. U.S.A. 95*, 11673−11678.
12. Arkin, I. T., Adams, P. D., MacKenzie, K. R., Lemmon, M. A., Brunger, A. T., and Engelman, D. M. (1994) *EMBO J. 13*, 4757−4764.
13. Patricelli, M. P., Lashuel, H. A., Giang, D. K., Kelly, J. K., and Cravatt, B. F. (1998) *Biochemistry 37*, 15177−15187.
14. Laage, R., Rohde, J., Brosig, B., and Langosch, D. (2000) *J. Biol. Chem. 275*, 17481−17487.
15. Furthmayr, H., and Marchesi, V. T. (1976) *Biochemistry 15*, 1137−1144.
16. Lemmon, M. A., Flanagan, J. M., Hunt, J. F., Adair, B. D., Bormann, B. J., Dempsey, C. E., and Engelman, D. M. (1992) *J. Biol. Chem. 267*, 7683−7689.
17. Lemmon, M. A., Flanagan, J. M., Treutlein, H. R., Zhang, J., and Engelman, D. M. (1992) *Biochemistry 31*, 12719−12725.
18. Fisher, L. E., Engelman, D. M., and Sturgis, J. N. (1999) *J. Mol. Biol. 293*, 639−651.
19. Reddy, L. G., Jones, L. R., and Thomas, D. D. (1999) *Biochemistry 38*, 3954−3962.
20. Fleming, K. G., Ackerman, A. L., and Engelman, D. M. (1997) *J. Mol. Biol. 272*, 266−275.
21. Langosch, D., Brosig, B., Kolmar, H., and Fritz, H. J. (1996) *J. Mol. Biol. 263*, 525−530.
22. Adair, B. D., and Engelman, D. M. (1994) *Biochemistry 33*, 5539−5544.
23. Li, M., Reddy, L. G., Bennett, R., Silva, N. D., Jones, L. R., and Thomas, D. D. (1999) *Biophys. J. 76*, 2587−2599.
24. Hunt, J. F., McCrea, P. D., Zaccai, G., and Engelman, D. M. (1997) *J. Mol. Biol. 273*, 1004−1019.
25. Leeds, J. A., and Beckwith, J. (1998) *J. Mol. Biol. 280*, 799−810.
26. Russ, W. P., and Engelman, D. M. (1999) *Proc. Natl. Acad. Sci. U.S.A. 96*, 863−868.
27. Mitsuoka, K., Hirai, T., Murata, K., Miyazawa, A., Kidera, A., Kimura, Y., and Fujiyoshi, Y. (1999) *J. Mol. Biol. 286*, 861−882.
28. Grigorieff, N., Ceska, T. A., Downing, K. H., Baldwin, J. M., and Henderson, R. (1996) *J. Mol. Biol. 259*, 393−421.
29. Luecke, H., Schobert, B., Richter, H. T., Cartailler, J. P., and Lanyi, J. K. (1999) *J. Mol. Biol. 291*, 899−911.
30. Sato, H., Takeda, K., Tani, K., Hino, T., Okada, T., Nakasako, M., Kamiya, N., and Kouyama, T. (1999) *Acta Crystallogr. D55*, 1251−1256.
31. Krebs, M. P., Li, W., and Halambeck, T. P. (1997) *J. Mol. Biol. 267*, 172−183.
32. Isenbarger, T. A., and Krebs, M. P. (1999) *Biochemistry 38*, 9023−9030.
33. Krebs, M. P., and Isenbarger, T. A. (2000) *Biochim. Biophys. Acta 1460*, 15−26.
34. Steele, J. C., Tanford, C., and Reynolds, J. A. (1978) *Methods Enzymol. 48*, 11−23.
35. Hayat, M. A. (1986) *Basic techniques for transmission electron microscopy*, Academic Press, Orlando, FL.
36. Dencher, N. A. (1986) *Biochemistry 25*, 1195−1200.
37. Sanders, C. R., and Landis, G. C. (1995) *Biochemistry 34*, 4030−4040.
38. Gabriel, N. E., and Roberts, M. F. (1984) *Biochemistry 23*, 4011−4015.
39. Sanders, C. R., and Prosser, R. S. (1998) *Structure 6*, 1227−1234.

40. Cassim, J. Y. (1992) *Biophys. J. 63*, 1432−1442.
41. Cherry, R. J., Muller, U., Henderson, R., and Heyn, M. P. (1978) *J. Mol. Biol. 121*, 283−298.
42. Heyn, M. P., Cherry, R. J., and Dencher, N. A. (1981) *Biochemistry 20*, 840−849.
43. Dencher, N. A., and Heyn, M. P. (1978) *FEBS Lett. 96*, 322−326.
44. Dencher, N. A., and Heyn, M. P. (1982) *Methods Enzymol. 88*, 5−10.
45. Stoeckenius, W., and Kunau, W. H. (1968) *J. Cell Biol. 38*, 337−357.
46. Andreu, J. M., and Timasheff, S. N. (1986) *Methods Enzymol. 130*, 47−59.
47. Koynova, R., and Caffrey, M. (1998) *Biochim. Biophys. Acta 1376*, 91−145.
48. Gabriel, N. E., and Roberts, M. F. (1986) *Biochemistry 25*, 2812−2821.
49. Oosawa, F., and Asakura, S. (1975) *Thermodynamics of the polymerization of protein*, Academic Press, London.
50. Huang, K. S., Bayley, H., and Khorana, H. G. (1980) *Proc. Natl. Acad. Sci. U.S.A. 77*, 323−327.
51. Lopez, F., Lobasso, S., Colella, M., Agostiano, A., and Corcelli, A. (1999) *Photochem. Photobiol. 69*, 599−604.
52. Woolf, T. B. (1998) *Int. J. Quantum Chem. 69*, 105−116.
53. Dowhan, W. (1997) *Annu. Rev. Biochem. 66*, 199−232.
54. Hoch, F. L. (1992) *Biochim. Biophys. Acta 1113*, 71−133.
55. Ioannou, P. V., and Golding, B. T. (1979) *Prog. Lipid Res. 17*, 279−318.
56. Zhou, Y., and Bowie, J. U. (2000) *J. Biol. Chem. 275*, 6975−6979.

BI0106585